FINITE ELEMENT METHOD AND NORMAL MODE MODELING OF CAPACITIVE MICROMACHINED SAW AND LAMB WAVE TRANSDUCERS

G.G. Yaralioglu*, F.L. Degertekin†, M.H. Badi*, B.A. Auld*, and B.T. Khuri-Yakub*

*Ginzton Laboratory, Stanford University, Stanford, CA 94305.
†Mechanical Engineering Dept., Georgia Institute of Technology, Atlanta, GA 30332.

Abstract— **Surface wave and Lamb wave devices without piezoelectricity are the latest breakthrough applications of the capacitive micromachined ultrasonic transducers (CMUTs). CMUTs were introduced for airborne and immersion applications. However, experiments showed that those devices couple energy not only to the medium but also to the substrate they are built on. By placing the CMUTs on a substrate in an interdigitated configuration, it is possible to couple energy to Lamb wave or Rayleigh wave modes with very high efficiency without a need for any piezoelectric material. In this study, we calculate the acoustic field distribution in silicon substrate as well as the acoustic impedance of the CMUT membrane, which includes the power coupled to the substrate. We apply the normal mode theory to find the distribution of the acoustic power among different Lamb wave modes. For low frequency (1 MHz) devices, we find that the lowest order antisymmetric (A_0) mode Lamb wave is the dominant mode in the substrate, and 95% of the power propagates through this mode. For high frequency devices (100 MHz), interdigital CMUTs excite Rayleigh waves with efficiencies comparable to piezoelectric surface acoustic wave (SAW) devices.**

Keywords— **Lamb Waves, Surface Acoustic Waves, Capacitive Ultrasonic Transducer.**

I. Introduction

Acoustic waves are being used in many sensor and filtering applications. Lamb wave based sensors have been demonstrated successfully in many areas as diverse as monitoring of chemical reactions, measurement of thin film thicknesses, detection of different gases [1]-[5]. Surface acoustic waves (SAWs) are mostly employed for filtering and analog signal processing applications [6], [7]. In all of these acoustic wave devices, ultrasonic waves are generated and detected by means of piezoelectric materials such as lead zirconium titanate, lithium niobate or zinc oxide. However, these piezoelectric materials are not compatible with the existing integrated circuit fabrication processes. This limits the integration of acoustic devices with the electronics on the same silicon wafer. Instead of piezoelectricity, using capacitive micromachined ultrasonic transducers (CMUTs) for generation and detection of acoustic waves in the substrate has greater potential for electronic integration. This results in inexpensive integrated circuits for mass production and devices with increased noise immunity because the cabling between the transducers and the electronics is eliminated.

CMUTs have been used to generate and detect ultrasonic waves only for liquid immersion and air-borne applications so far [8]-[10]. A CMUT consists of a metalized silicon nitride membrane supported by posts, and it is built on a silicon wafer using standard micromachining techniques. The electrode on the membrane and the highly doped silicon substrate form a parallel plate capacitor which is used to generate and detect ultrasonic waves in the immersion medium. When a voltage is applied between the metalized membrane and the substrate, electrostatic forces attract the membrane towards the substrate. Stress within the membrane and the bending stiffness of the membrane resist the attraction. Driving the membrane with a time harmonic signal generates acoustic waves in the immersion medium. Since the electrostatic forces are always attractive, for a sinusoidal motion, a bias voltage should be added to the ac drive. CMUTs can also be used for the detection of ultrasound. A biased membrane under an impinging acoustic field can generate significant currents.

The CMUT membranes are generally considered clamped at their edges, and most of the previous work has focused on the interaction of the membrane and the ultrasonic waves in the immersion medium. However, recent experiments have shown that these devices couple energy also to the substrate. Radiation pattern measurements in liquid media clearly identified the leaky Lamb wave propagation in the substrate due to vibrating CMUT membranes [11]. The coupling between the membranes and the silicon substrate occurs through the membrane supports. In this paper, we present devices that are optimized for coupling energy into the particular Lamb wave propagation mode of the substrate. We will use finite element analysis and normal mode decomposition to find the power coupled to the different waveguide modes.

II. Device Geometry

Figure 1 shows one element of the transducer. Many of these membranes are used together to form the complete device. The fabrication process is the same as that of circular CMUTs [10], the only difference is that the membrane is rectangular. The metal electrode covers half of the membrane area, and its thickness is negligible compared to the thickness of the membrane. The substrate is a highly doped 500-μm thick (100) silicon wafer. The long dimension of the membrane is perpendicular to the $< 110 >$ crystal axis. This crystal axis chosen to be the direction of the Lamb wave or SAW propagation since it has the minimum diffraction loss [12]. Below 5 MHz, for a 500-μm thick silicon wafer, the only propagating Lamb wave modes are the lowest order A_0 and S_0 modes [13]. For low frequency

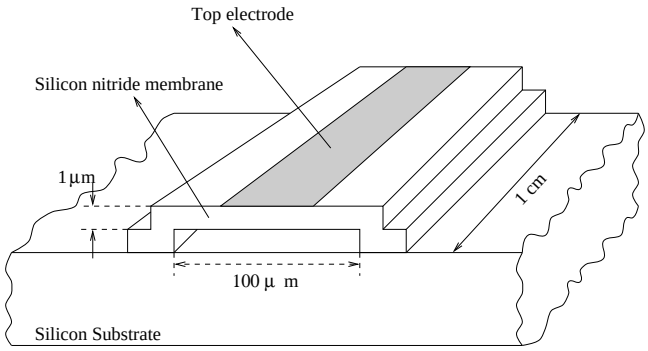

Fig. 1. Single rectangular membrane.

operation, membrane dimensions are 100 μm and 1 cm as indicated in Fig. 1. The thickness of the membrane and the air gap are both 1 μm. The width and the thickness of the membrane with the residual stress determine the resonance frequency. For the above values, the resonance frequency is approximately 1.2 MHz assuming a 100 MPa residual stress in the silicon nitride membrane. The long dimension of the membrane is much larger than the acoustic wave length in the substrate, so that the membrane can be considered as a plane wave source in this direction.

The complete transducer is shown in Fig. 2. The device is analogous to an interdigital piezoelectric transducer, with the piezoelectric material replaced by vibrating membranes. The finger width and the spacing are $\lambda/4$ and λ, respectively, where λ is the acoustic wavelength in the substrate. Each finger is composed of many membranes, the $\lambda/4$ finger width is filled with as many membranes as possible to increase the efficiency of the device. In the figure, the receiver is composed of only one membrane. However, it can be populated with membranes like the transmit fingers for increased efficiency.

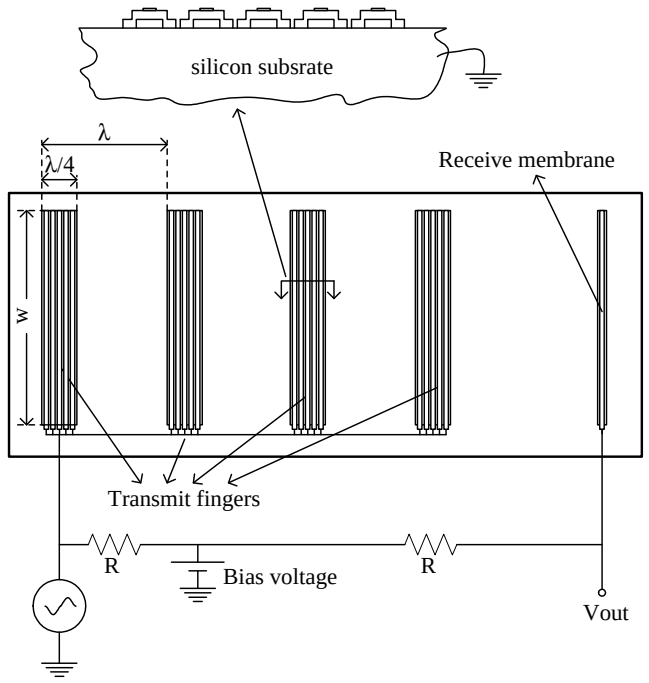

Fig. 2. Lamb wave or SAW device.

III. FEM and Normal Mode Analysis

We performed finite element (FE) calculations[1] and normal mode decomposition [12], [14] to identify the propagating modes in the substrate for the single membrane shown in Fig. 1. The FE mesh is depicted in Fig 3. The structure is symmetric with respect to the Y axis, hence, symmetric boundary conditions are applied on this axis. We assume uniform and time harmonic electrostatic forces on the membrane electrode as shown in the figure. Two dimensional calculations are carried out since the length of the membrane is substantially larger than its width.

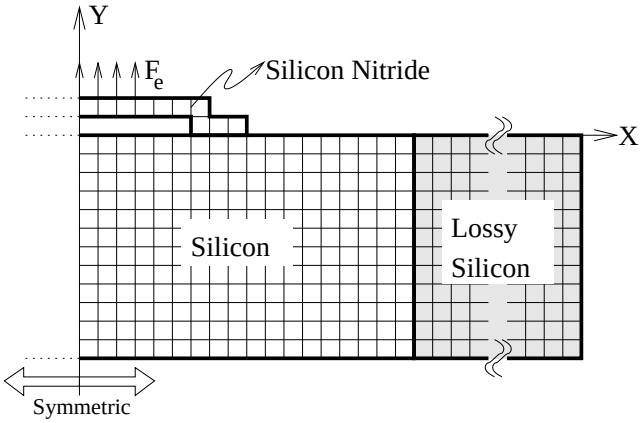

Fig. 3. Finite element mesh of the CMUT.

In the above model, to be able to characterize wave propagation in the substrate, one needs absorbing boundaries at the ends of the silicon wafer. We use a lossy silicon region of considerable length at the silicon ends to absorb the impinging fields [15], [16]. We keep the loss coefficient in the lossy part as small as possible so that the standing wave pattern on the silicon surface due to the reflections from the silicon/lossy-silicon interface is negligible. The length of the lossy part is adjusted so that the fields inside attenuate before the reflections from the lossy-silicon end reach to the silicon. We also keep the mesh size as small as possible to avoid very long computation times.

We used the structure in Fig. 3 to run harmonic analyses. The FE analysis provided the particle displacement and stress distribution across the thickness of the silicon wafer generated by the harmonic excitation of the membrane. We apply normal mode decomposition to the FE results. Normal mode analysis suggests that any arbitrary velocity field $\mathbf{v}(x,y)$ and associated stress $\mathbf{T}(x,y)$ distribution can be expressed as a sum of the normal modes as [12], [14]

$$\mathbf{v}(x,y) = \sum_{n=0}^{\infty} a_n(x)\mathbf{v}_n(y) \tag{1}$$

$$\mathbf{T}(x,y) = \sum_{n=0}^{\infty} a_n(x)\mathbf{T}_n(y).\hat{\mathbf{x}} \tag{2}$$

[1] ANSYS5.6 is used for FEM calculations.

where $a_n(x)$ are the normal mode amplitudes. $\mathbf{v}_n(x,y)$ and $\mathbf{T}_n(x,y)$ are the normal velocity and stress distributions, respectively[2]. For the model in Fig. 3, the following velocity and stress components are considered: v_x, v_y, T_{xx} and T_{xy}. Hence, the normal mode amplitude for an arbitrary field distribution is given by

$$a_n = -\frac{1}{4P_{nn}} \int_{-h}^{0} (v_{x_n}^* T_{xx} + v_{y_n}^* T_{xy} + v_x T_{xx_n}^* + v_y T_{xy_n}^*) \mathrm{d}y \tag{3}$$

where the average normal mode power P_{nn} per unit length is

$$P_{nn} = -\frac{1}{2} \mathcal{R}e \left\{ \int_{-h}^{0} (v_{x_n}^* T_{xx_n} + v_{y_n}^* T_{xy_n}) \mathrm{d}y \right\} \tag{4}$$

The above equations are evaluated at $x = x_1$ where x_1 is in the silicon region just before the silicon/lossy silicon interface. Finally, the average propagating power in mode n is

$$P_n = |a_n|^2 P_{nn} \tag{5}$$

For low frequency thickness products, the only propagating Lamb wave modes are A_0 and S_0. Hence, the membrane in Fig. 1 generates only these two modes in the silicon substrate. Calculated relative power at each mode is depicted in Fig. 4. The resonance frequency is 1.26 MHz where the propagating power is maximum. It is evident that most of the power (more than 95%) is coupled to the A_0 mode. As the frequency increases S_0 becomes more significant. The quality factor of the resonance curves in Fig. 4 is relatively large (> 10000). Note that, for the above calculation we assumed that membrane is in vacuum.

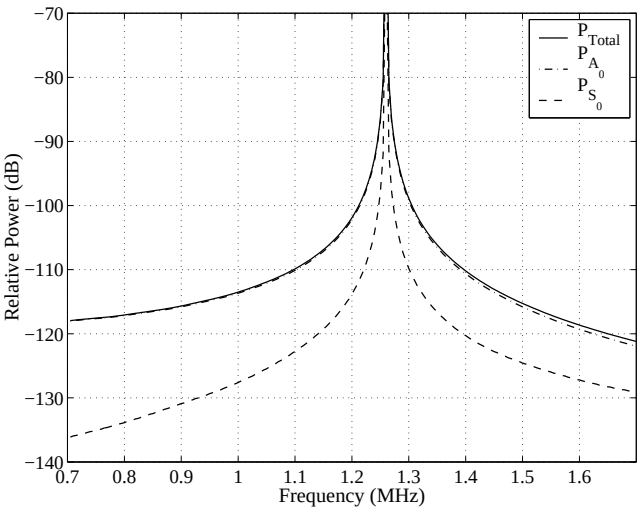

Fig. 4. Relative power at each mode for the membrane depicted in Fig. 1. Residual stress in the silicon nitride membrane is 100 MPa.

From the above analysis, we calculate the radiation resistance and incorporate this value into an equivalent circuit model of the CMUT. The ideal lossless membrane can be modeled by a series combination of an inductor and a capacitor. The radiation resistance will be added to this model in series. The impedance of the membrane can be calculated by

$$Z_m = \frac{F_e}{\bar{v}} \tag{6}$$

where F_e is the applied structural force on the electrode and the $\bar{v}$ is the average velocity of the membrane calculated by FE analysis. If there were no loss, Z_m would be purely imaginary which can be modeled by an LC-circuit. However, wave propagation in the substrate results in a real part. Moreover, the real part of the membrane impedance can be divided into two parts representing the radiation resistance of A_0 and S_0 given by

$$R_n = \frac{2P_n}{|\bar{v}|^2} \tag{7}$$

Calculated resistances are depicted in Fig. 5. In the graph, the plane wave air impedance of 100 μm by 1 cm membrane is also plotted for comparison purposes. Figure 5 suggests that if this device operates in air, most of the power will radiate into air and a small amount will propagate in the waveguide modes. Hence, for maximum efficiency, these devices should be operated in vacuum.

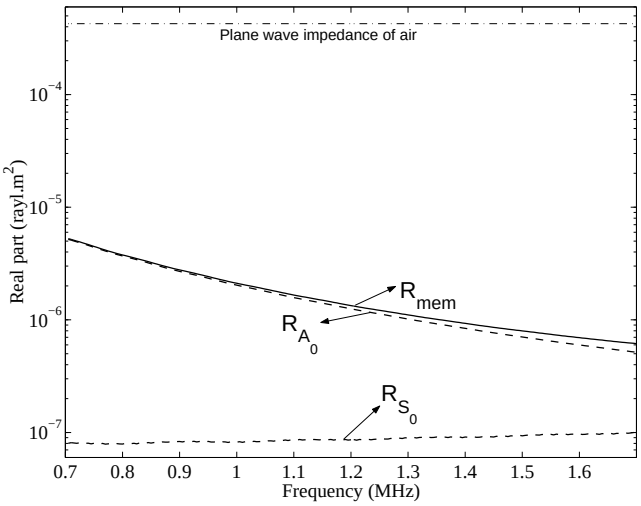

Fig. 5. Real part of radiation impedance for single CMUT membrane

The bandwidth of the CMUT Lamb wave or SAW transducers is determined by the membrane resonances. By using the devices on 0.5 mm thick silicon wafer it is possible to construct very high-Q filters. However, most of the sensor and filtering applications require bandwidth control. Hence, we investigated the mechanisms that could alter the bandwidth of the membrane resonance. First, we calculated the quality factors of membranes with different support shapes. Our FEM and normal mode results showed that the effect of the support shape is minimal. Second, we changed the substrate thickness. The quality factor of the membrane resonance as a function of thickness is shown in Fig. 6. With decreasing thickness, the quality factor decreases whereas the radiation impedance increases. Hence,

[2]Normal velocity distribution for Lamb waves are given in reference [12]. Normal stress fields can be calculated from equation of motion.

it is possible to control the bandwidth and to increase the coupling into the substrate by reducing the substrate thickness.

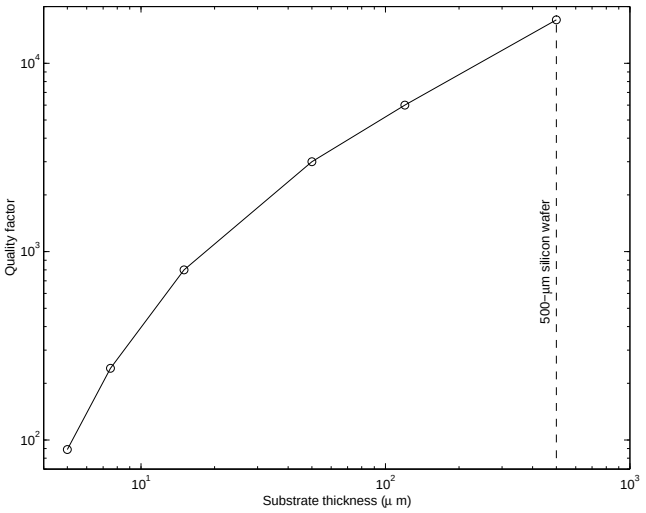

Fig. 6. Quality factor as a function of substrate thickness.

We also applied our analysis to the SAW devices in the vicinity of 100 MHz. In this case, the membrane width is 10 μm. The SAW wavelength in the $< 110 >$ direction is around 50 μm. The result is depicted in Fig. 7. The peaks at 98 MHz and 107 MHz correspond to the reflection of longitudinal waves from the bottom of the wafer. Although the plot does not reveal a clean resonance shape, it can be deduced that the quality factor of the membrane resonance is around 100, which suggests that SAW excitation efficiency is relatively high, and the power coupled into the SAW is approximately 1/10 of the total power resulting in a 10 dB insertion loss. The rest of the power propagates in higher order waveguide modes and bulk waves.

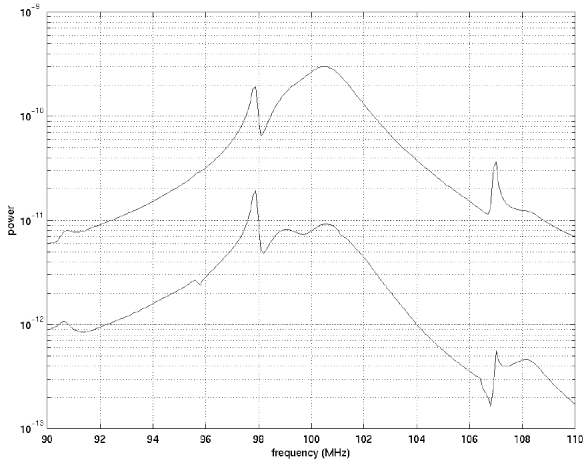

Fig. 7. Propagating power in SAW device.

Conclusion

The distinct advantage of CMUT Lamb wave and SAW devices is that fabrication of the transducer is fully compatible with IC manufacturing processes. The resulting transducer will be inexpensive and can be integrated easily with electronic devices. In this study, we demonstrated the FEM and normal mode analysis of new CMUT based transducers. We found that for low frequency devices A_0 is the dominant mode and at high frequencies, these devices can excite Rayleigh waves with high efficiency. Another unique property of CMUT transducers is that the bandwidth of the device is determined by the quality factor of the membrane resonances. The bandwidth and the quality factor can be adjusted by changing the substrate thickness.

Acknowledgments

This work was supported by the Office of Naval Research.

References

[1] A.J. Ricco, S.J. Martin, "Acoustic wave viscosity sensor," *Appl. Phys. Let.*, Vol. 50, p. 1474, 1987.

[2] S.W. Wenzel and R.M. White, "A multisensor employing and ultrasonic Lamb wave oscillator," *IEEE Trans. Electron Devices* Vol. 35, p. 735, 1988.

[3] M.J. Vellekoop, G.W. Lubking, P.M. Sarro and A. Venema, "Integrated-circuit-compatible design and technology of acoustic-wave-based microsensors," *Sensors Actuators A*, Vol. 44, p. 249, 1994.

[4] D.F. Fischer, W.J. Varhue, J. Wu and C.A. Whiting, "Lamb wave microdevices fabricated on monolithic single crystal silicon wafers," *Journal of Microelectromechanical systems*, Vol. 9, No. 1, p. 88, 2000.

[5] E. Moulin, J. Assaad, C. Delebarre, H. Kaczmarek and D. Balageas, "Piezoelectric transducer embedded in a composite plate: Application to Lamb wave generation," *J. Appl. Phys.*, Vol. 82, p. 2049, 1997.

[6] G.S. Kino, *Acoustic Waves: Devices, Imaging, &Analog Signal Processing*, Prentice-Hall, Inc., New Jersey, 1987.

[7] C.K. Campbell, *Surface Acoustic Wave Devices for Mobile and Wireless Communications*, Academic Press Inc., San Diego, 1998.

[8] M.I. Haller and B.T. Khuri-Yakub, "A surface micromachined electrostatic ultrasonic air transducer," *IEEE Trans. Ultrason. Ferroelect., Freq. Contr.*, Vol. 43, pp. 1-6, Jan. 1996.

[9] H.T. Soh, I. Ladabaum, A. Atalar, C.F. Quate and B.T. Khuri-Yakub, "Silicon micromachined ultrasonic immersion transducers," *Appl. Phys. Lett.*, Vol. 69, pp. 3674-3676, Dec. 1996.

[10] I. Ladabaum, X. Jin, H.T. Soh, A. Atalar, B.T. Khuri-Yakub, "Surface micromachined capacitive ultrasonic transducers," *IEEE Trans. on UFFC*, Vol 45, pp. 678-690, May 1998.

[11] X.C. Jin, F.L. Degertekin, S. Calmes, X.J. Zhang, I. Ladabaum and B.T. Khuri-Yakub, "Micromachined capacitive transducer arrays for medical ultrasound imaging," *IEEE Ultrasonics Symposium Proceedings*, p. 1877, 1998.

[12] B.A. Auld, *Acoustic Fields and Waves in Solids*, Vol 2, John Wiley and Sons, Toronto, 1973.

[13] I.A. Viktorov, *Rayleigh and Lamb Waves: Physical Theory and Applications*, Plenum Press, New York, 1967.

[14] F.L. Degertekin, B.T. Khuri-Yakub, "Single mode Lamb wave excitation in thin plates by Hertzian contacts," *Appl. Phys. Lett.*, Vol. 69, pp. 146-148, 1996.

[15] E. Moulin, J. Assaad, C. Delebarre and D. Osmont, "Modeling of Lamb waves generated by integrated transducers in composite plates using coupled finite element-normal modes expansion method," *J. Acoust. Soc. Am.*, Vol. 107, pp. 87-94, Jan. 2000.

[16] A. Bozkurt, F.L. Degertekin, A. Atalar and B.T. Khuri-Yakub, "Analytic modeling of loss and cross-coupling in capacitive micromachined ultrasonic transducers," *IEEE Ultrasonics Symposium Proceedings*, pp. 1025, 1998.